Autonomous Homing of Parafoil and Payload System Based on ADRC

Liang Jiao*. Qinglin Sun*. Xiaofeng Kang. Zengqiang Chen *, Zhongxin Liu ***

°* Department of Automation, School of Information Technology, Nankai University, Tianjin, China, (e-mail: jiaoliang@mail.nankai.edu.cn, sunql@nankai.edu.cn, chenzq@nankai.edu.cn, lzhx@nankai.edu.cn)
** Military Representative Office of Aerospace Industries Ltd, Hubei, China, (e-mail: kz0426@mail.nankai.edu.cn)

Abstract A High-glide system, parafoil-based, allows for a safe steady delivery as well as interference penetration. Based on the background of the parafoil and air-drop robot system in disaster environment, the horizontal trajectory tracking is considered to meet the requirement of landing precision. The control scheme includes tracking the setting trajectory, using cross track error algorithm and Active Disturbance Rejection Control (ADRC). First, the position and heading information are obtained according to the six degrees-of-freedom parafoil and payload kinematics model. Then the heading guidance is designed according to cross track error. Finally, the heading controller is devised based on ADRC and control value is saturated to protect the system from peaking in the observer's transient response. The validity of the control algorithm in applying to the trajectory tracking is confirmed in the simulation. The results show that the controller design can achieve high precision on tracking control and has better dynamic performance than PD controller.

Keywords: parafoil and payload system, Active Disturbance Rejection Control (ADRC), cross track error, saturate, trajectory tracking.

1. INTRODUCTION

Parafoil has a lot of applications in aircraft recovery and equipment delivery because of its perfect control and glide performance (Wang, 1997; Xiong, 2005; N. Slegers et al., 2004; N. Slegers et al., 2009), which can greatly improve air-drop precision and quality. Once a disaster happens, the parafoil and air-drop robot system will be delivered into the disaster scene. The public safety and technology standards in the disaster reduction field can be upgraded by means of various probing sensors carried by robot.

Operation of the parafoil and payload system is affected by the deflection of left and right parafoil brakes. The system turns left, while left manipulating rope is pulled down by the motor, and vice versa. Through constantly motor control, the setting trajectory will be tracked. If there is no proper error correction used in the control system, precise autonomous homing cannot be achieved. Therefore, the control strategy is the key to autonomous homing of the parafoil and payload system. Many different control strategies have been developed for autonomous homing of the parafoil and payload system (Xiong, 2005; N. Slegers et al., 2004; N. Slegers et al., 2009). Nathan Slegers (N. Slegers et al., 2004) studied a maneuver using model predictive control. A reduced state linear model based on a nonlinear six degrees-of-freedom is established. The desired trajectory in the horizontal plane is mapping into a desired heading angle using Lagrange interpolating polynomials. Then the reduced state linear model is used for model predictive control.

Currently, the Active Disturbance Rejection Control (ADRC), invented by J Han (Han, 2009), is being applied to a wide variety of problems, spanning many different domains. Qing Zheng (Qing et al., 2007) developed the ADRC for driving the drive axis of MEMS gyroscope to resonance and regulating the output amplitude of the axis to a fixed level. Mingwei Sun (Mingwei et al., 2010) applied the ADRC to the flight attitude control. The design of ship tracking controller (Jiuhong et al., 2008) was investigated by utilizing ADRC method. The results show that the controller can achieve high precision and has strong robustness to controlled plant parameter perturbations and environment disturbances.

Our study adopts ADRC to the horizontal trajectory tracking control of the parafoil and payload system. The six degrees-of-freedom kinematics model provides the system position and attitude. The current heading angle is obtained through the system position, while the desired heading angle is computed based on setting trajectory. Finally the saturated ADRC heading controller is devised to the system.

2. SIX DEGREES-OF-FREEDOM PARAFOIL AND PAYLOAD KINEMATICS MODEL

The model of the parafoil and payload system has been widely studied (Wang, 1997; Xiong, 2005; N. Slegers et al., 2004; N. Slegers et al., 2009). It is modeled as a rigid structure with six degrees-of-freedom in this paper, which includes three inertial positions as well as three Euler orientations of the system mass center. Fig.1 shows schematic of the dynamic system that consists of a parafoil canopy connected to a payload object. O_{sys} is the mass center, and P is the apparent mass center of payload in the parafoil and payload system reference frame. $O_{sys}X_{sys}Y_{sys}Z_{sys}$ is the body reference frame of the parafoil and payload system, while $O_eX_eY_eZ_e$ is the inertial frame.

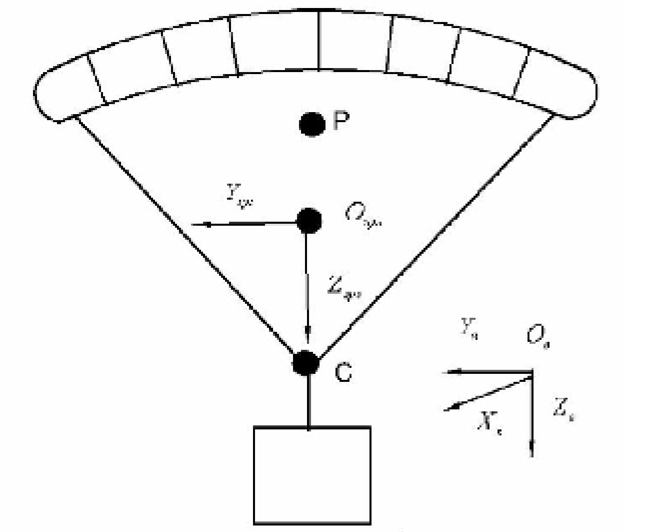

Fig. 1. Front view of six degrees-of-freedom parafoil and payload system.

$$\begin{bmatrix} \dot{x} \\ \dot{y} \\ \dot{z} \end{bmatrix} = TR_{e-sys}^{T} \begin{bmatrix} v_x \\ v_y \\ v_z \end{bmatrix} \tag{1}$$

In equation (1), x, y, z represent components of position vectors of mass center O_{sys} in an inertial frame, and v_x, v_y, v_z are components of velocity vectors of mass center. The matrix TR_{e-sys} represents the transformation matrix from the inertial reference to the body reference frame.

$$TR_{e-sys} = \begin{bmatrix} c_\theta c_\psi & c_\theta s_\psi & -s_\theta \\ s_\zeta s_\theta c_\psi - c_\zeta s_\psi & s_\zeta s_\theta s_\psi + c_\zeta c_\psi & s_\zeta c_\theta \\ c_\zeta s_\theta c_\psi + s_\zeta s_\psi & c_\zeta s_\theta s_\psi - s_\zeta c_\psi & c_\zeta c_\theta \end{bmatrix} \tag{2}$$

For any angle σ, $\sin(\sigma) \equiv s_\sigma$ and $\cos(\sigma) \equiv c_\sigma$ exist, that mean the shorthand notation for trigonometric function. The transformation matrix is determined by three Euler angles, that is, roll ζ, pitch θ, and yaw ψ.

$$\begin{bmatrix} \dot{\zeta} \\ \dot{\theta} \\ \dot{\psi} \end{bmatrix} = \begin{bmatrix} 1 & s_\zeta t_\theta & c_\zeta t_\theta \\ 0 & c_\zeta & -s_\zeta \\ 0 & s_\zeta c_\theta^{-1} & c_\zeta c_\theta^{-1} \end{bmatrix} \begin{bmatrix} w_x \\ w_y \\ w_z \end{bmatrix} \tag{3}$$

Where, w_x, w_y, and w_z are the angular velocity of the parafoil and payload system in the body reference frame.

In equation (4), A_{11} is the sum of intrinsic and apparent mass about the system mass center, A_{22} is the combination of intrinsic and apparent inertia, and $A_{12} = -A_{21}^{T}$ is the coupling of velocity and moment (or angular velocity and force).

$$\begin{bmatrix} \dot{v}_x \\ \dot{v}_y \\ \dot{v}_z \\ \dot{w}_x \\ \dot{w}_y \\ \dot{w}_z \end{bmatrix} = \begin{bmatrix} A_{11} & A_{12} \\ A_{21} & A_{22} \end{bmatrix}^{-1} \begin{bmatrix} F \\ M \end{bmatrix} \tag{4}$$

$$F = f_F(m_{sys}, p_h, S_W, S_P, C_L, C_D, v, W_{ind}) \tag{5}$$

$$M = f_M(m_{sys}, p_{h_{ight}}, S_W, S_P, C_L, C_D, v, W_{ind}, L_l, L_W) \tag{6}$$

Where, m_{sys} is the total mass of parafoil and payload system, $p_{h_{ight}}$ is the air density of $p_{h_{ight}}$ vertical height, S_W is the resistance features area of payload, S_P is the area of parafoil canopy, C_L and C_D are the parafoil canopy drag coefficient and lift coefficient, $v = [v_x, v_y, v_z]$ is the velocity of mass center in body reference frame, W_{ind} is velocity vector of wind, L_l and L_W are the canopy cord and sling.

$$C_L = f_L(\alpha, \delta_e, \delta_a) \tag{7}$$

$$C_D = f_D(\alpha, \delta_e, \delta_a) \tag{8}$$

Where, α is the angle of incidence, δ_e is lateral control, and δ_a is collective control. Lateral control is obtained by differential deflection while collective control is created by mutual deflection of the left and right side parafoil brakes.

3. COMPOSITION OF ADRC CONTROLLER AND SATURATE THE CONTROL VALUE

Many control objects model can be simplified as follows (Han, 2009),

$$\begin{aligned} \ddot{x} &= f(x, \dot{x}, \omega_{dtr}, t) + b_0(t)u(t) \\ y &= x \end{aligned} \tag{9}$$

Where, ω_{dtr} is external disturbance variable, $u(t)$ is control input, $b_0(t)$ is magnification factor, $f(x, \dot{x}, \omega_{dtr}, t)$ is the internal disturbances function. For the two-order system, its standard ADRC controller is as (Fig.2).

The ADRC controller consists of two main parts: "Extended State Observer (ESO)" and "Feedback Control Law (FCL)" (Fig.2). Where, $v_0(t)$ is the setting point, $z_1(t)$ is the estimation of output $y(t)$, $z_2(t)$ is the differential of output, and $z_3(t)$ is the estimation of the $f(x, \dot{x}, \omega_{dtr}, t)$, $e(t)$ is the error, $u_0(t)$ is the output of FCL, b_0 is the estimation $b_0(t)$, and $sat()$ is the standard saturation function.

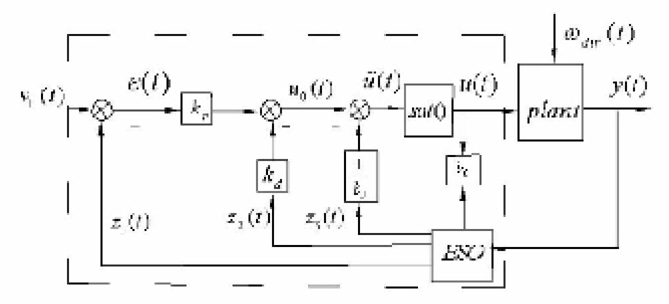

Fig. 2. The Structure of ADRC Controller for Two-Order System.

3.1 The Extended State Observer (ESO)

The main purpose of ESO is to be an extended state space model (9) that includes f shorthand notation for $f(x, \dot{x}, \omega_{dtr}, t)$, as an additional state.

$$\begin{aligned} x_1 &= y \\ x_2 &= \dot{y} \\ x_3 &= f \end{aligned} \tag{10}$$

Rewrite (9) in the extended state space,

$$\begin{aligned} \dot{x} &= Ax + Bu + Eh \\ y &= x_1 \end{aligned} \tag{11}$$

With,

$$A = \begin{bmatrix} 0 & 1 & 0 \\ 0 & 0 & 1 \\ 0 & 0 & 0 \end{bmatrix}, B = \begin{bmatrix} 0 \\ b \\ 0 \end{bmatrix}, E = \begin{bmatrix} 0 \\ 0 \\ 1 \end{bmatrix} \tag{12}$$

Where, h is the derivation of f. Then, the following linear discrete observer is used to estimate the state x.

$$\begin{aligned} \dot{z} &= Az + Bu + L(y - \hat{y}) \\ \hat{y} &= z_1 \end{aligned} \tag{13}$$

The observer gain $L = [b_1, b_2, b_3]$ is selected appropriately. Equation (13) provides an estimate of the state of (9). The ESO in its original form employs nonlinear observer gains. By choosing linear gains, this observer is denoted as the linear extended state observer. The observer gains are parameterized as (Gang et al., 2007),

$$L = [3\omega_0, 3\omega_0^2, \omega_0^3] \tag{14}$$

In which ω_0 is the only tuning parameter, standing for the observer bandwidth. The observer state z_3 will excellently track x_3 if the bandwidth is well tuned.

3.2 The ADRC Control Law and Synthesis of Control Value

The control law is illustrated as,

$$u_0(t) = k_p(v_0 - z_1) - k_d z_2 \tag{15}$$

$$u(t) = (u_0(t) - z_3) / b_0 = \tilde{u}(t) \tag{16}$$

$$\begin{gathered} \ddot{y} = x_3 + b_0((u_0(t) - z_3) / b_0) \\ \Updownarrow \\ \ddot{y} = (x_3 - z_3) + u_0(t) \approx u_0(t) \end{gathered} \tag{17}$$

Equation (15) is the so called Feedback Control Law (FCL). The controller tuning can be simplified with $k_d = 2\omega_c$ and $k_p = \omega_c^2$ (Gang et al., 2007). The combination of (13) and (15) is considered as the parameterized ADRC.

3.3 Saturate the Control Value

The ESO (13) can be made to coincide with the system (9) by taking (16). However, the control value (16) must be saturated to protect the system from peaking in the observer's transient response (Leonid et al., 2008). Let

$$M > \max \left| \frac{u_0(t)}{b_0} \right| \tag{18}$$

Where, M be the maximal control value of the motor.

$$u(t) = M\ sat\left(\frac{b_0 \tilde{u}(t)}{M}\right) \tag{19}$$

4. HORIZONTAL TRAJECTORY TRACKING ALGORITHM BASED ON ADRC

Heading guidance and controller are two key elements in horizontal trajectory tracking problem of the parafoil and payload system. According to the horizontal deviation between current position and setting trajectory of the system, heading guidance is computed. Then the desired heading is given by heading guidance. As the heading of the system manipulated through the heading controller, the system movement will track the setting trajectory.

4.1 Heading Guidance Design Based on Cross Track Error

In order to minimize the trajectory tracking error, heading guidance is designed which is based on cross track error (Tang, 2009; Yeonsik et al., 2009). Fig.3 shows horizontal trajectory schematics of the parafoil and payload system. The calculation method of cross track error is described as follows.

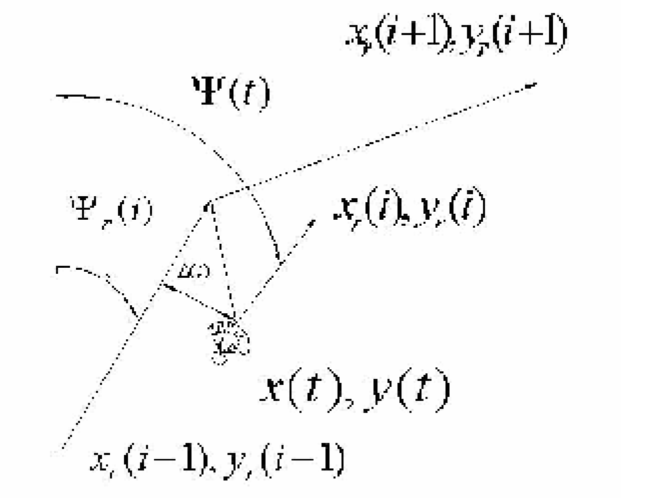

Fig. 3. Horizontal Trajectory Tracking Schematics of Parafoil and Payload System.

$$\begin{aligned} \Delta x &= x_r(i) - x_r(i-1) \\ \Delta y &= y_r(i) - y_r(i-1) \\ \hat{x} &= x_r(i) - x(t) \\ \hat{y} &= y_r(i) - y(t) \end{aligned} \tag{20}$$

Where, $(x_r(i), y_r(i))$ and $(x_r(i-1), y_r(i-1))$ are the current trajectory point and the former, and $(x(t), y(t))$ is t**he current position of the parafoil and payload system.**

The distance between $(i-1)_{th}$ trajectory point and i_{th} is given in (21).

$$L_i = \sqrt{\Delta x^2 + \Delta y^2} \tag{21}$$

The trajectory tracking error and heading angle of tracking line are given in (22) and (23) respectively.

$$\Delta(t) = (\hat{x}\Delta y - \hat{y}\Delta x) / L_i \tag{22}$$

$$\Psi_{tr}(i) = \tan^{-1}(\Delta y / \Delta x) \tag{23}$$

The desired heading angle based on the trajectory tracking error and heading angle of tracking line is described as (24).

$$\Psi_r(t) = k_\Delta \Delta(t) + \Psi_{tr}(i) \tag{24}$$

The tracking error of heading angle $\Psi_e(t)$ is equivalent to $\Psi_r(t) - \Psi(t)$. Then the trajectory tracking problem of the parafoil and payload system is converted to the heading tracking problem.

4.2 Controller Design Based on ADRC

The current heading angle of parafoil and payload system $\Psi(t)$ is given in (25).

$$\Psi(t) = \tan^{-1}\left(dx/dy|_t\right) \tag{25}$$

$$\begin{aligned} d\Psi/dt|_t &= w_z(t) \\ dw_z/dt|_t &= f(\Psi(t), w_z(t)) + \omega_{dtr}(t) + b_0(t)u(t) \end{aligned} \tag{26}$$

With unknown disturbance type, equation (26) can be rewritten as,

$$\begin{aligned} \ddot{\Psi}|_t &= f(\Psi(t), w_z(t)) + \omega_{dtr}(t) + b_0(t)u(t) \\ y &= \Psi(t) \end{aligned} \tag{27}$$

With the ESO (13) properly designed, the control value $u(t)$ is calculated through (15) and (16), which is equal to lateral brake deflection δ_e in (6) and (7). Force F and moment M in (5) and (6) will change with δ_e. And then heading angle will change with $[\dot{w}_x, \dot{w}_y, \dot{w}_z]^T$ in (4). Finally heading control in the parafoil and payload system is realized.

5. SIMULATION RESULTS

5.1 Simulation Conditions

The kinematics model of the six degrees-of-freedom parafoil and payload system presented in this paper is established based on Matlab.

According to mass constraint of the air-drop robot (about $80kg$), simulation conditions are set as Table 1.

Table 1. Parameters of parafoil canopy

Description	Variable and value	Description	Variable and value
Parafoil canopy Area	$S_P = 22m^2$	Aspect ratio	$\lambda = 1.73$
Rigging angle	$\phi = 7^\circ$	Canopy cord	$L_l = 3.7m$
Canopy sling	$L_W = 0.5m$	Payload mass	$m_W = 80kg$
Payload resistance features area		$S_W = 0.5m^2$	

The original values of kinematics equation are given as,

The original velocities are $[v_x, v_y, v_z]_0^T = [15.9, 0, 2.1]^T$.

The original Euler angles are $[\zeta, \theta, \psi]_0^T = [0, 0, 0]^T$.

The original angular velocities are $[w_x, w_y, w_z]_0^T = [0, 0, 0]^T$.

Set the simulation time and ESO sampling time as 0.1s. Set the control cycle as 2s. In the autonomous homing of parafoil and payload system, the percentage of manipulate rope scrolled by the motor must limit itself to a conservative bound. The saturation parameter M is 0.139. The observer gains of three-order ESO are parameterized as (14), observer bandwidth is $\omega_0 = 2$.

5.2 Comparative Simulation Between the ADRC and PD Control

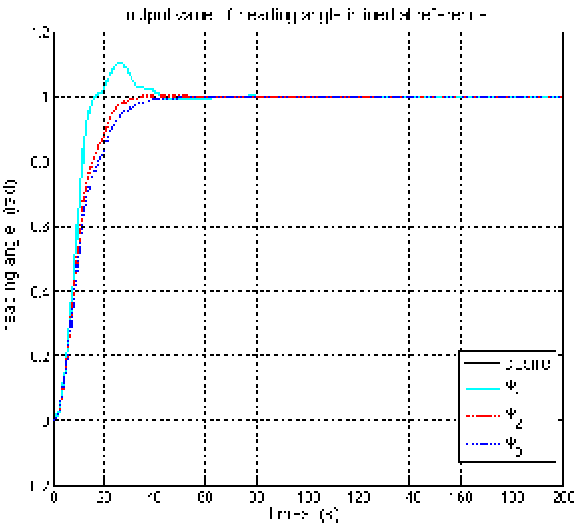

Fig. 4. Output value of heading angle in inertial reference (ADRC).

Compared with the response in Fig.4, the performance of the system with ADRC is affected by the variations of b_0. Control parameters are shown as follows, $k_p = 0.07$, $k_d = 0.20$, $b_0 = 0.5$ (Solid line Ψ_1), $b_0 = 0.2$ (dot dash line Ψ_2), $b_0 = 0.1$ (dotted line Ψ_3). The compensation z_3 to the system changes with the magnification factor b_0. When $b_0 = 0.5$, the adjusting time is 14s, while $b_0 = 0.1$, the adjusting time is 40s. The output (Ψ) is more stable because of the output shock cut by appropriate disturbance compensation. The control value changes smoothly, which favours the actuator and energy conservation (Fig.5).

Compared with the response in Fig.4 (ADRC) and in Fig.6 (PD), the control parameters of ADRC are $k_p = 0.07$, $k_d = 0.20$ and $b_0 = 0.5$, while the PD are $k_p = 0.07$, $k_d = 0.20$ (dotted line Ψ_2), $k_p = 0.09$, $k_d = 0.20$ (solid line Ψ_1).

When ADRC is used, the adjusting time is 20s, without output, while PD control, the adjusting time 42s, with output shock. Adjusting time can be improved with control parameters increasing, but this will make the system unstable.

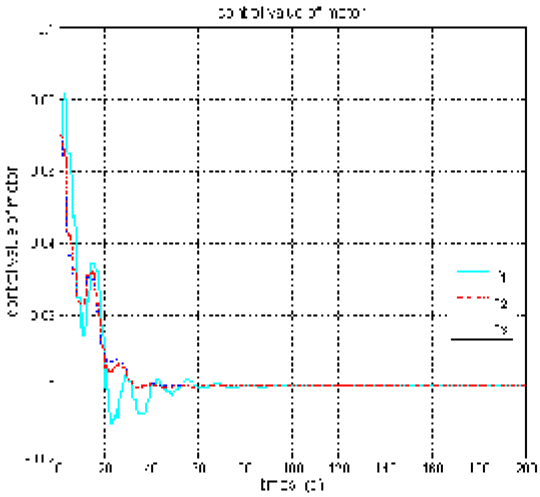

Fig. 5. Control value of motor (ADRC).

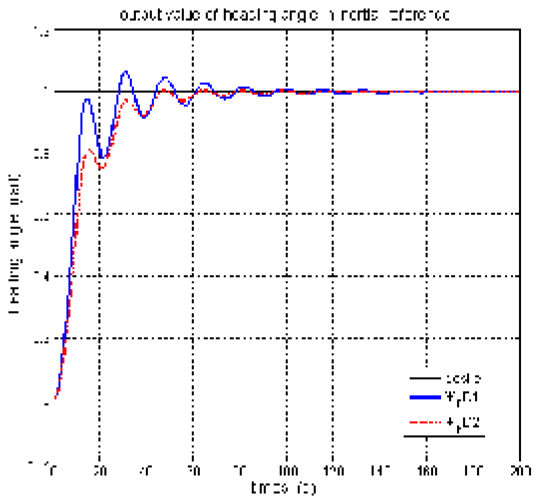

Fig. 6. Output value of heading angle in inertial reference (PD).

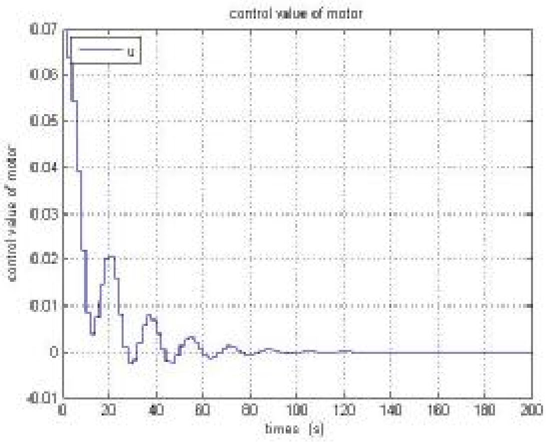

Fig. 7. Control value of motor (PD).

5.3 Trajectory Tracking Simulation Examples

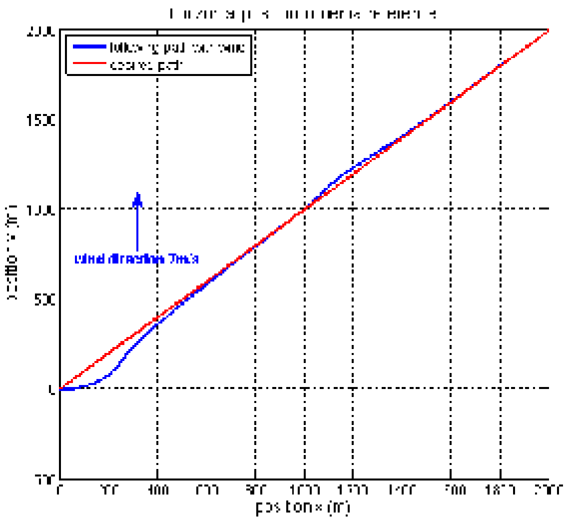

Fig. 8. Following straight trajectory in inertial reference (ADRC).

The desired straight trajectory for the system is decided by $(0,0),(2000,2000)$. The trajectory of the system is shown using ADRC with $k_p = 0.07$, $k_d = 0.20$, $b_0 = 0.5$, $k_\Delta = -0.0018$ (Fig.7). The trajectory of the ADRC, represented by a solid line, converged to the desired trajectory (Fig.8).

When it is bigger than the heading deviation, the position deviation plays a key role in heading guidance. The system tracks the heading guidance and follows the desired trajectory within 20s. The constant wind disturbance is imposed as $W_{ind\_y} = 7m/s$ in the moment of 100s to observe the effect of the uncertainty in the trajectory tracking. The system deviates from the desired trajectory. The heading angle of the system is adjusted under the function of ADRC controller.

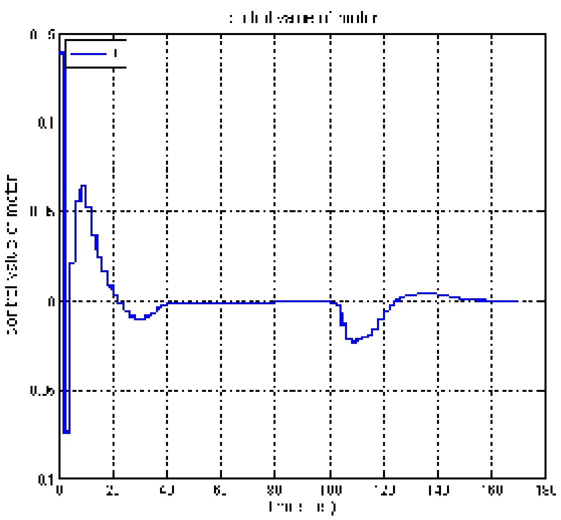

Fig. 9. Straight trajectory control value of motor (ADRC).

Fig. 9 shows the control value of motor using the ADRC. The control value is small, and the manipulation runs well and smoothly.

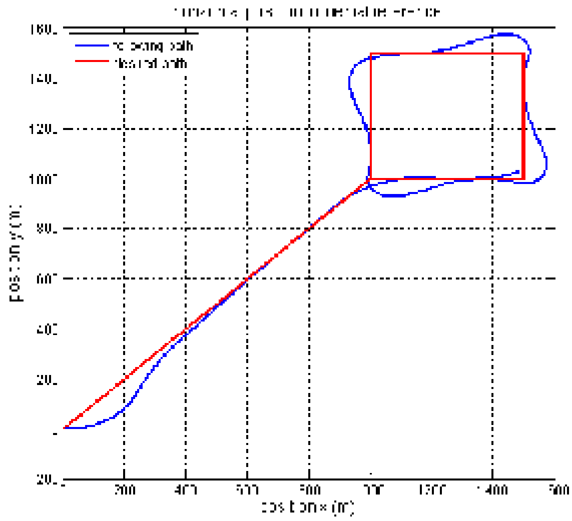

Fig.10. Following square trajectory in inertial reference (ADRC).

As shown in Fig.10, the desired square trajectory for the system is $(0,0),(1000,1000)$, $(1500,1000)$, $(1500,1500)$, $(1000,1500)$ .The simulation intends to evaluate the performance of the ADRC in the case of switching. A large deviation in inflection point exists, which is due to the restrictions of the system turning rate. The above simulation results show that the designed control scheme is effective.

6. CONCLUSION

This paper has presented a method for improving autonomous homing of the parafoil and payload system based on ADRC. The state estimation and compensation of the change of system parameters and outside disturbance are implemented by ESO and FCL. The saturated control value is to protect the system from peaking. The ADRC produces better dynamic performance than the PD controller. The process of heading angle tracking the guidance is fast, smooth, and with very low energy consumption. Simulation results show that the proposed algorithm is simple, effective and can greatly improve the performance of the system. It is indicated that such a scheme can be applicable to practical parafoil and payload system.

ACKNOWLEDGEMENTS

This work was supported in part by Major Program of Tianjin Science Foundation under Grant 10JCZDJC15900, Tianjin Key Technology R&D Program grant number 09ZCKFSF00500, and Program for New Century Excellent Talents in University grant number NCET-10-0506.

REFERENCES

Dongchul Yoo, Stephen S. -T. Yau, Fellow(2006). On Convergence of the Linear Extended State Observer.

Proceedings of the 2006 IEEE International Symposium on Intelligent Control Munich, Germany, October 4-6, 2006

Gang Tian, and Zhiqiang Gao. (2007). Frequency response analysis of active disturbance rejection based control system. *In 16th IEEE International Conference on Control Applications Part of IEEE Multi-conference on Systems and Control*, 1595-1599.

Jaroslaw Hajduk, Andrzej Moldenhower, and Krzysztof Sibilski. (2007). Experimental validation of mathematical model of autonomous gliding delivery system. *In 19th AIAA Aerodynamic Decelerator Systems Technology Conference and Seminar*, 2571-2586.

Jingqing Han. (2009). From PID to active disturbance rejection control. *IEEE Transactions on Industrial Electronics*, 56(3), 900-906.

Jiuhong Ruan, Zuowei Li, Fengyu Zhou, and Yibin Li. (2008). ADRC based ship tracking controller design and simulations. *Proceedings of the IEEE International Conference on Automation and Logistics*, 1763-1768.

Leonid B, and Hassan K. Khalil. (2008). Performance recovery of feedback-linearization-based designs. *IEEE Transactions on Automatic Control*, 53(10), 2324-2334.

Mingwei Sun, Ruiguang Yang, and Zengqiang Chen. (2010). Flight active disturbance rejection control design and performance analysis. *Proceedings of the 8th World Congress on Intelligent Control and Automation*, 765-770.

N. Slegers, and M. costello. (2004). Model predictive control of a parafoil and payload system. *In 13th AIAA Atmospheric Flight Mechanics Conference and Exhibit,* 4822-4858.

N. Slegers, and O. Yakimenko. (2009). Optimal control for terminal guidance of autonomous parafoils. *In 20th AIAA Aerodynamic Decelerator Systems Technology Conference and Seminar*, 2958-2978.

Qing Zheng, Lili Dong, and Zhiqiang Gao. (2007). Control and rotation rate estimation of vibrational MEMS gyroscopes. *In 16th IEEE International Conference on Control Applications Part of IEEE Multi-conference on Systems and Control*, 118-123.

Tang Li. (2009). *Research on the neural network adaptive control for autonomous underwater vehicle's horizontal tracking problem,*62-67. Harbin Engineering University, Harbin, China.

Wang Lirong. (1997). *Parachute theory and application,* 528-600. Astronautic Publishing House, Beijing, China.

Xiong Jing. (2005). *Research on the dynamics and homing project of parafoil system,* 97-123. National University